

# Simulation of crack propagation in porous compacted specimens of aspirin

R. C. ROWE, R. J. ROBERTS

ICI Pharmaceuticals, Alderley Park, Macclesfield, Cheshire, SK10 2NA, UK

A model originally developed to simulate crack propagation in structural steel has been evaluated for porous compacted specimens of aspirin. The fracture mechanism is assumed to consist of hole growth and coalescence. The program allows both visualization of crack growth and the calculation of crack velocity. Simulations to investigate the effect of stress intensity factor indicate that the critical stress intensity factor for sustained growth for aspirin is of the order of  $0.15 \text{ MPa m}^{1/2}$  consistent with experimental findings. The program is easy to use enabling many simulations to be performed with minimum effort.

## Nomenclature

$a$	Polar coordinate with origin at the crack tip
$C_d$	Propagation velocity of the irrotational wave
$E$	Young's modulus of elasticity
$H$	Indentation hardness
$K$	Stress intensity factor at the crack tip
$K_{IC}$	Critical stress intensity factor
$n$	The exponent
$R$	Radius of the hole/pore
$t$	Time
$V$	Crack-tip velocity
$\beta$	Fluidity (i.e. the reciprocal of the viscosity)
$\delta$	The smoothening length
$\theta$	Polar coordinate with origin at the crack tip
$\rho$	True density
$\sigma$	Stress
$\sigma_0$	Flow or yield stress
$\nu$	Poisson's ratio

## 1. Introduction

Pharmaceutical materials used in tableting vary in their deformation behaviour from those that are brittle and consolidate by particle fragmentation to those that are ductile and consolidate by plastic flow. Whilst considerable attention has been directed to the study of compaction behaviour of such materials, characterization has, in general, been constrained by techniques selected to reflect their end-use, e.g. pressure–volume relationships obtained using instrumented presses. However, recent studies have demonstrated the applicability of a fracture mechanics approach using porous specimens to determine critical stress intensity factors [1–4]. Such studies have focused on the need to understand crack propagation in porous specimens and although some work has been attempted in this area [5], results have been constrained by the techniques adopted, e.g. high-speed photography. An approach found useful in structural steels is that of computer simulation [6, 7] and, although developed as a simple demonstration of crack

growth where propagation is by hole growth and coalescence, the model described would appear applicable to porous specimens of compacted powders [8]. In this work a model has been evaluated for porous specimens of aspirin prepared by compaction.

## 2. The model

For a detailed description of the model, the reader is recommended to consult the papers by Broberg [6, 7]. There are six essential features of the model

1. The model assumes a plane case where holes in the specimen are assumed to be cylindrical. Their sizes are determined after a Gaussian distribution with a variable standard deviation (expressed as a fraction of the mean). The position of the holes is randomly distributed.

2. Hole growth occurs according to a viscosity rule [6]

$$\frac{1}{R} \left( \frac{dR}{dt} \right) = \beta \left( \frac{\sigma}{\sigma_0} - 1 \right)^2 \left[ 1 + \left( \frac{\sigma}{\sigma_0} - 1 \right)^n \right] \quad (1)$$

where  $\sigma$ , the stress, is always greater than  $\sigma_0$ , the flow or yield stress of the material,  $R$  represents the radius of the hole,  $t$  is time,  $\beta$  is the fluidity (i.e. the reciprocal of the viscosity) of the material, and  $n$  is an exponent.

3. The stress is assumed to be scalar and is given by the expression

$$\sigma = \frac{K}{[\pi(a + \delta)]^{1/2} + (\pi a)^{1/2}} \times \left[ \frac{(1 - (V^2/C_d^2) \sin^2 \theta)^{1/2} + \cos \theta}{1 - (V^2/C_d^2) \sin^2 \theta} \right]^{1/2} \quad (2)$$

where  $K$  is the stress intensity factor at the crack tip,  $V$  represents the crack tip velocity,  $C_d$  is the propagation velocity of the irrotational wave  $a$  and  $\theta$  correspond to the polar coordinates with their origin at the crack tip, and  $\delta$  is the so-called smoothening length introduced to remove singularity [7].

4. Holes are opened when the stress reaches a critical value dependent on the size of the hole.

5. Hole coalescence occurs when the distance between two holes (or one hole and the main crack) becomes smaller than a certain critical distance given by the expression  $1.25(R_i + R_j)$  where  $R_i$  and  $R_j$  are the radii of holes  $i$  and  $j$  respectively.

6. Hole opening and growth causes a stress reduction in the neighbourhood of the crack.

The simulation has been written in both Quick-BASIC and Turbo C for a personnel computer [7, 9]. Holes are displayed on the computer screen as circles scaled to include one hundred holes and growth by drawing a new periphery for each step. Coalescence and crack formation between two holes is simply indicated by a straight line between the centres of the holes.

### 3. Experimental procedure

The program asks for an input of average hole diameter, volume fraction, values for the yield stress, fluidity, exponent, irrotational wave velocity and stress intensity factor. Unfortunately, accurate values for all the parameters are not available but it is possible to estimate them based on previously published data for aspirin.

#### 3.1. Hole size and volume fraction

Pore (hole) sizes and volume fractions for compressed specimens of aspirin have been measured by high-pressure mercury intrusion porosimetry [10]. Data from this work have shown that aspirin powder compacted to 105 MPa forms a compact with a porosity of 6.45% and a mean pore diameter of  $0.24 \mu\text{m}$  with a range of  $0.08\text{--}0.4 \mu\text{m}$ .

#### 3.2. Yield stress, $\sigma_0$

An accurate value of the yield stress,  $\sigma_0$ , of a material can be obtained from indentation hardness,  $H$ , values using the expression

$$\sigma_0 = \frac{H}{3} \quad (3)$$

Hence, an indentation hardness value of 87 MPa [11] results in a yield stress for aspirin of 29 MPa.

#### 3.3. Fluidity, $\beta$

The fluidity of an organic material like aspirin will be very high compared to that for steel ( $1000 \text{ s}^{-1}$  [7]). However, it can be estimated by multiplying the value for steel by the ratio of the Young's modulus of elasticity of steel (200 GPa) to that of aspirin (7.5 GPa [12]). This results in a value for the fluidity of aspirin of  $26700 \text{ s}^{-1}$ .

#### 3.4. Irrotational wave velocity, $C_d$

This parameter can be calculated using the expression [9]

$$C_d = \left[ \frac{E}{(1 - \nu^2)\rho} \right]^{1/2} \quad (4)$$

where  $E$  is the Young's modulus of elasticity,  $\nu$  is Poisson's ratio and  $\rho$  is the true density of the material. Using values of 7.5 GPa [12], 0.3 [13] and  $1400 \text{ kg m}^{-3}$ , respectively, for aspirin yields an irrotational wave velocity of  $2426 \text{ m s}^{-1}$ .

#### 3.5. Exponent, $n$

The exponent,  $n$ , is related to the sensitivity of the material to over stress. For steel, Broberg [7] has

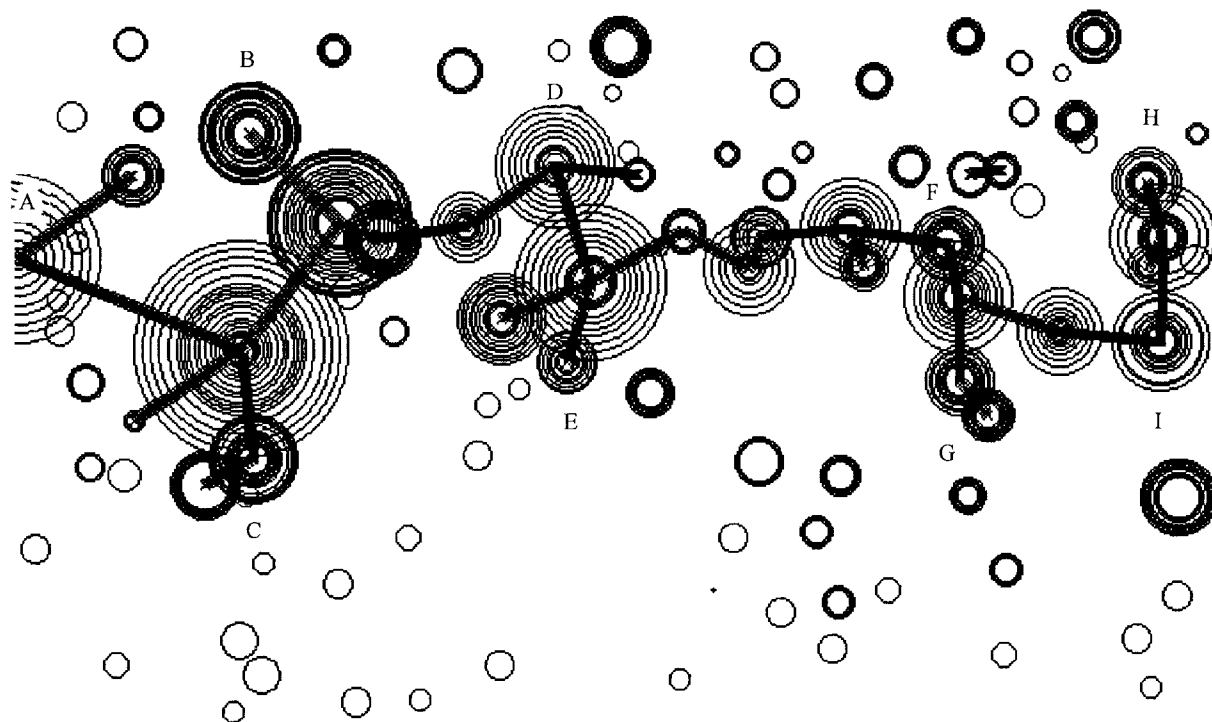


Figure 1 A simulation of cracking in an aspirin compact of 6.5% porosity containing pores  $0.24 \pm 0.024 \mu\text{m}$  diameter at a stress intensity factor of  $0.15 \text{ MPa m}^{1/2}$ . Simulation programmed to start at A. Note conchoidal cracks BC, DE, FG, HI.

assumed a value of 4, but for organic materials such as aspirin it will be significantly lower. For the purposes of this paper  $n$  has been taken as unity, a value shown to be acceptable for other organic materials such as microcrystalline cellulose [8] and hydroxypropyl methylcellulose [14, 15].

### 3.6. Stress intensity factor, $K$

This parameter has been measured for aspirin using single-edge notched beams [4]. However, because one of the objectives of the work is to estimate a value for  $K_{IC}$ , the critical stress intensity factor for sustained crack growth from simulations, to compare it to

actual measurements, this parameter was left as a variable.

## 4. Observations

### 4.1. Crack propagation and velocity

Fig. 1 illustrates a simulation for a porous compact with a porosity of 6.5 % and mean pore (hole) size of  $0.24 \mu\text{m}$  (standard deviation  $\pm 0.024 \mu\text{m}$ , i.e. 10 % of mean) assuming a stress intensity factor of  $0.15 \text{ MPa m}^{1/2}$ . In this as in all other simulations, the crack has been programmed to start at point A. The features seen in the simulation, a non-linear major

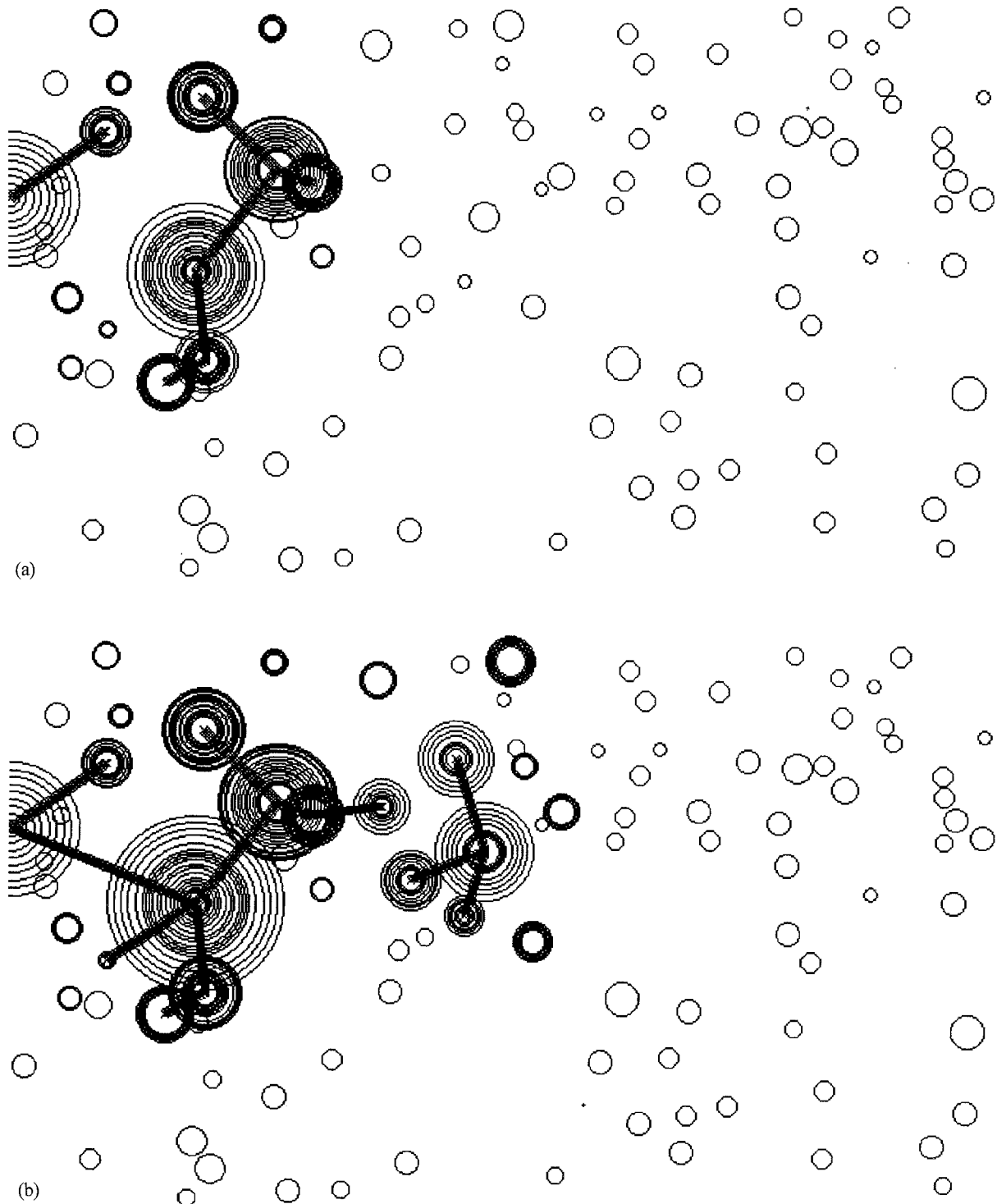


Figure 2 Simulations showing the development of conchoidal cracks in systems as described in Fig. 1.

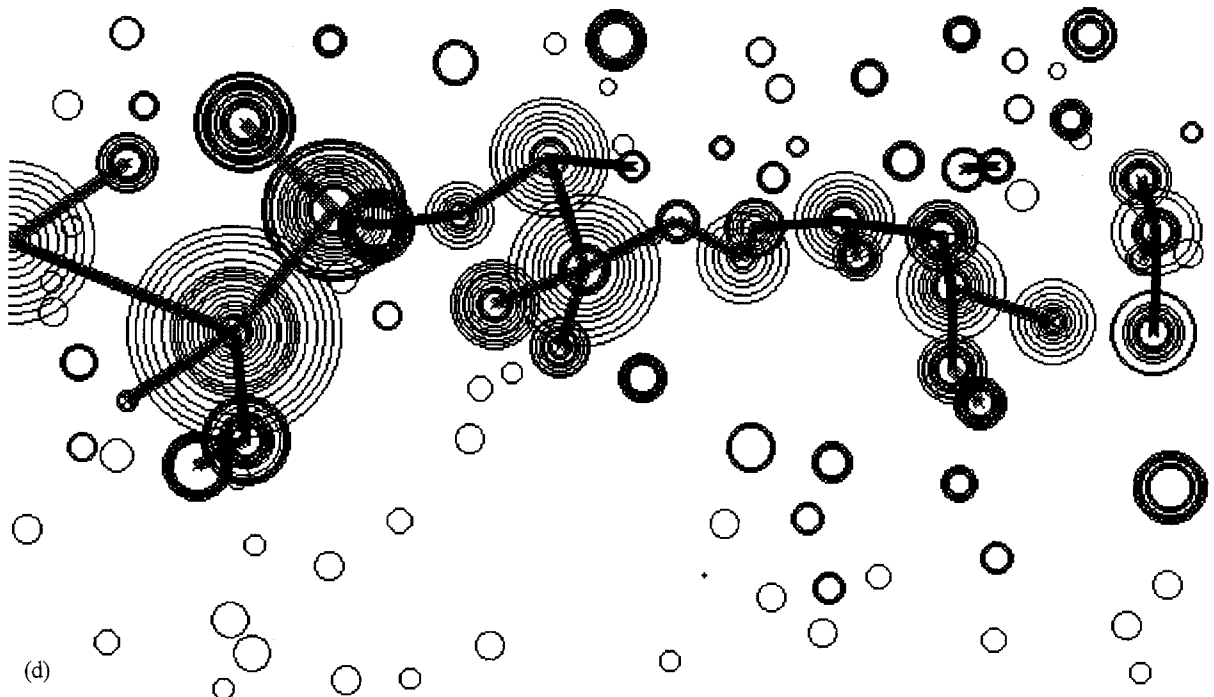
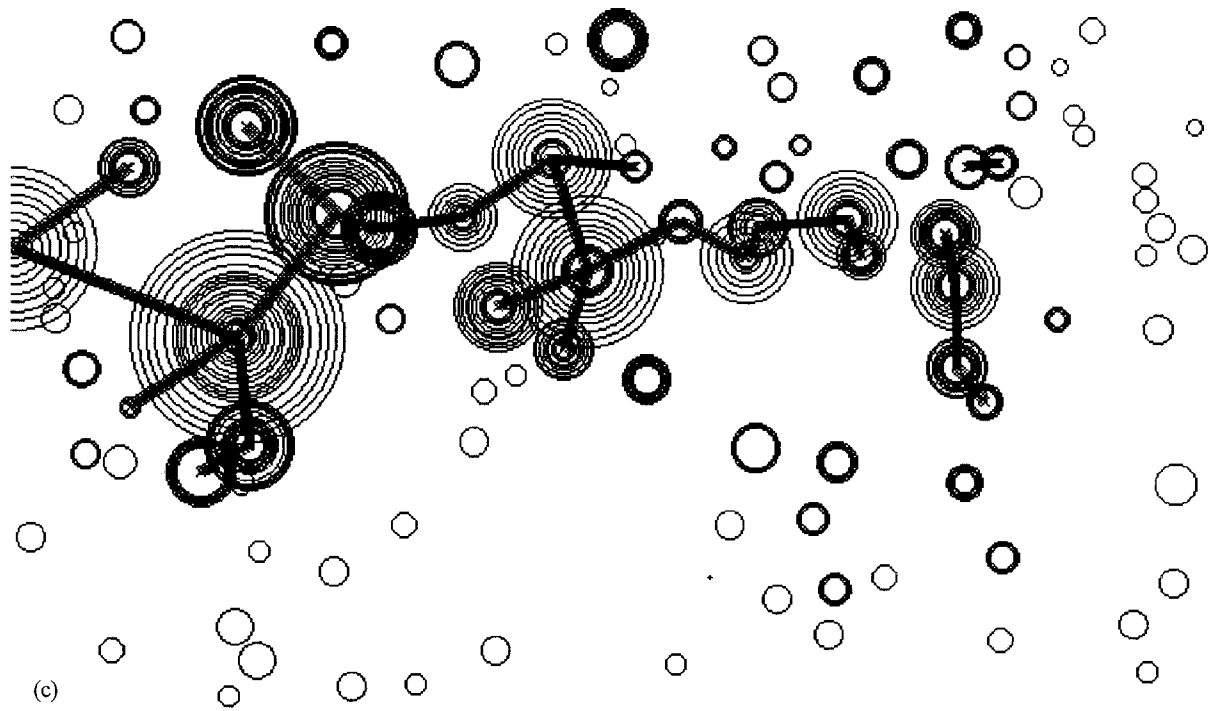


Figure 2 contd. (c, d).

crack with smaller branch cracks, are often found in compacted porous specimens when observed under the scanning electron microscope [12]. An interesting feature is the apparent concentricity of the branch cracks (BC, DE, FG, HI) seen on the simulation. Investigation of the progress of crack growth by the use of a screen capture program (Fig. 2) shows the initial formation of conchoidal cracks which then link with the main crack. This is consistent with experimental observations during surface hardness measurements on aspirin with a Vickers indenter [11].

It should be noted that any calculations, e.g. for crack velocities and critical stress intensity factors, from simulations will only be approximate because of

the randomized distribution of the holes and the routine which corrects for the possibility of overlapping holes inherent in the computer program. However, it is possible to gain some insight into the degree of variation by performing repeat simulations with the same input parameters but different randomizations. Fig. 3 shows the results (mean and standard deviations of seven randomizations) for the calculation of crack velocities at various stress intensity factors for the system with a porosity of 6.5 %, mean pore (hole) size of  $0.24 \mu\text{m}$  with both zero standard deviation (i.e. monosized) and a standard deviation of 50 % of the mean, i.e.  $\pm 0.12 \mu\text{m}$ . In all cases the coefficient of variation in crack velocities was less than 40 %.

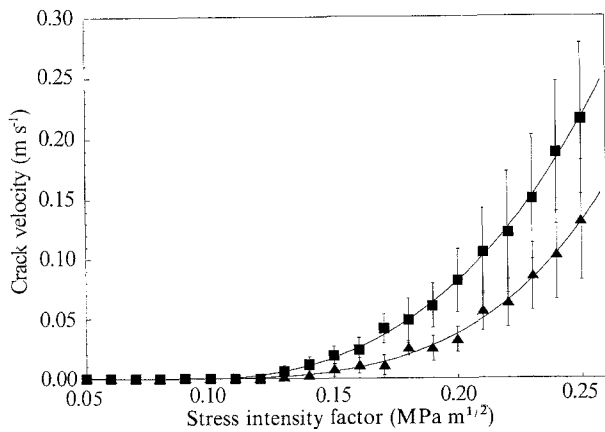


Figure 3 Crack velocity versus stress intensity factor for compacts of aspirin of 6.5% porosity containing pores  $0.24 \mu\text{m}$  diameter with (■) 0% standard deviation (i.e. monosized) (▲) 50% standard deviation.

#### 4.2. Estimation of $K_{IC}$ of aspirin

Fig. 4 illustrates a simulation equivalent to the one shown in Fig. 1 but with a stress intensity factor of  $0.25 \text{ MPa m}^{1/2}$ . It is immediately apparent that increasing the stress intensity factor results in the formation of a different crack route and the appearance of a number of small cracks independent of the main crack. There is also an increase in crack velocity,  $0.284 \text{ ms}^{-1}$ , compared to  $0.011 \text{ ms}^{-1}$  at the lower stress intensity factor of  $0.15 \text{ MPa m}^{1/2}$ . There is still some evidence of concentricity AB, CD, EF, GH, but not as pronounced as seen at the lower stress intensity factor.

Fig. 5 illustrates a simulation equivalent to that shown in Fig. 1 both with an increased standard deviation

of pore (hole) size of 40% of the mean, i.e.  $\pm 0.10 \mu\text{m}$ . This simulation has been chosen because pore size distribution data on aspirin tablets using mercury intrusion porosimetry [10] would suggest an experimental standard deviation of between 10% and 20% of the mean with an absolute maximum of 40%. This change results in the formation of a different crack route, a smaller number of branch cracks diverging from the main crack and an absence of cracks independent of the main crack. No evidence of concentricity can be seen but the crack velocity is similar to that seen in the simulation with the standard deviation of 10% of the mean (Fig. 1), i.e.  $0.086 \text{ ms}^{-1}$ .

The critical stress intensity factor needed for substantial crack growth for aspirin can be found by pooling data from repeated simulations. Figs. 3 and 6 show such data. It can be seen that, irrespective of the standard deviation of the mean pore (hole) size there is no substantial growth, below a stress intensity factor of 0.15 but above this figure crack growth is sustained with a velocity of  $0.01\text{--}0.02 \text{ ms}^{-1}$ . Hence it can be concluded that the critical stress intensity factor for aspirin is  $0.15 \text{ MPa m}^{1/2}$  in agreement with experiment,  $0.156 \text{ MPa m}^{1/2}$ , determined using single-edge notched beam [4].

#### 5. Conclusion

Despite the fact that the program contains many simplifications of a very complex phenomenon, the agreement with experiment both qualitatively and quantitatively for aspirin is extremely good. The program is very easy to use enabling many simulations to be performed with minimum effort.

It must be realized that the model is based on continuum rather than contact mechanics and hence

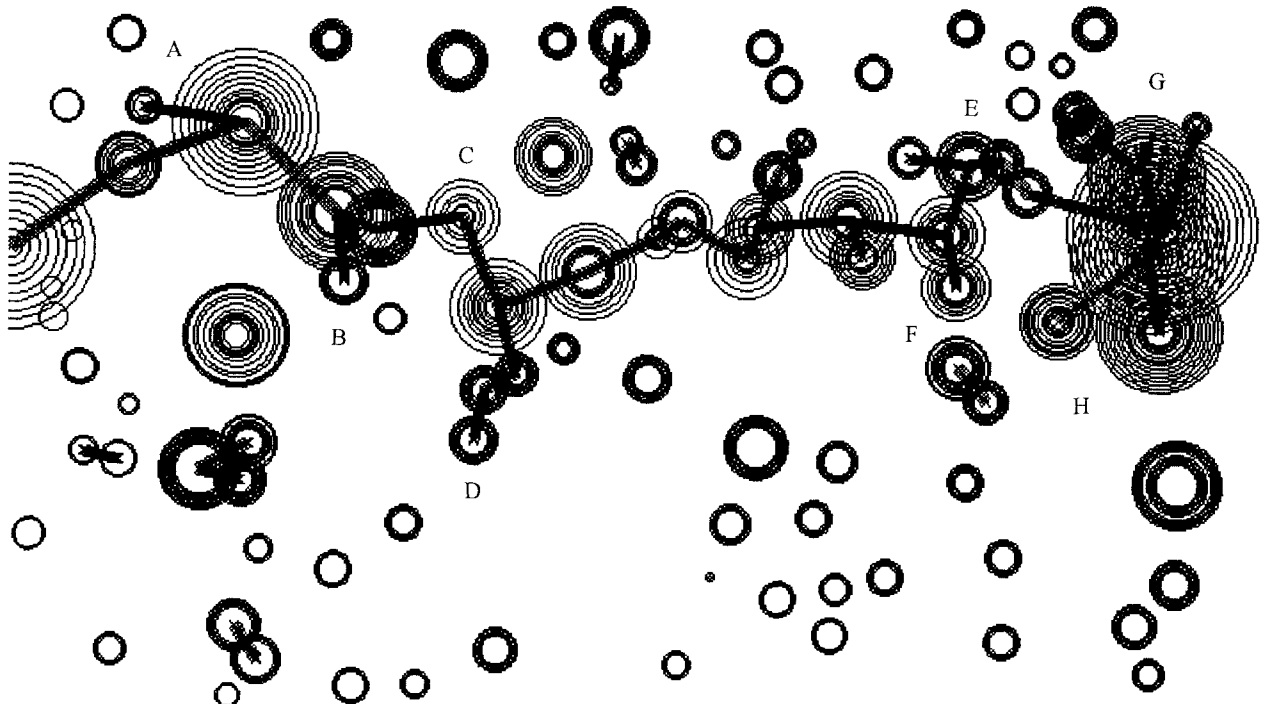


Figure 4 Simulation of cracking in an aspirin compact of 6.5% porosity containing pores  $0.24 \pm 0.024 \mu\text{m}$  diameter at a stress intensity factor of  $0.25 \text{ MPa m}^{1/2}$ .

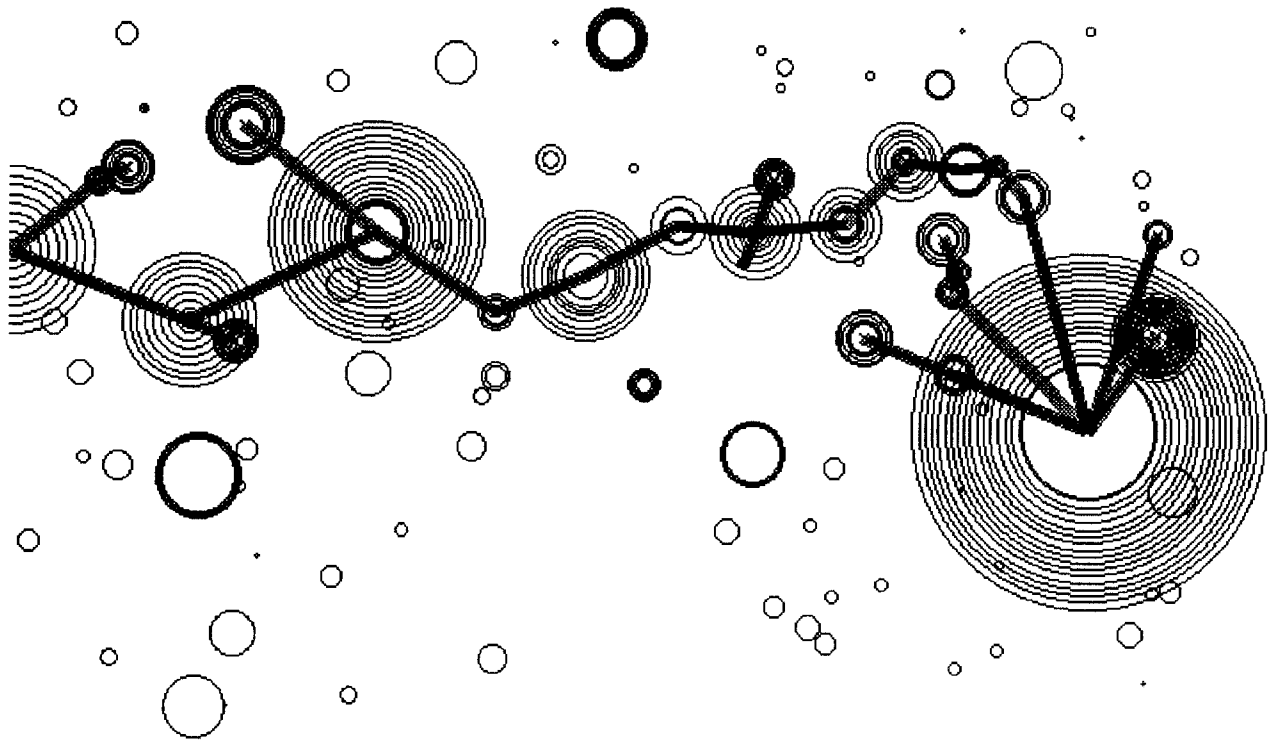


Figure 5 A simulation of cracking in an aspirin compact of 6.5% porosity containing pores  $0.24 \pm 0.10 \mu\text{m}$  diameter at a stress intensity factor of  $0.15 \text{ MPa m}^{1/2}$ .

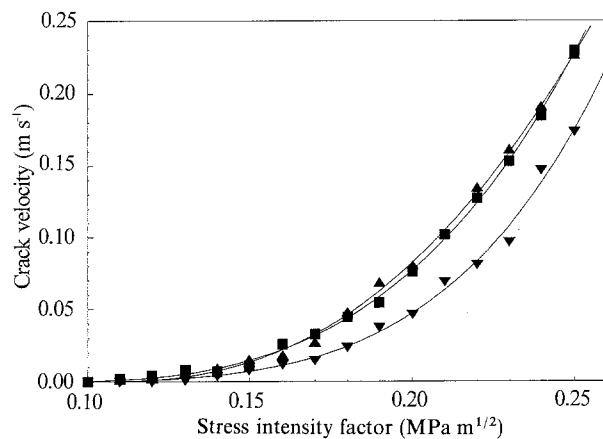


Figure 6 Crack velocity versus stress intensity factor for compacts of aspirin of 6.5% porosity containing pores  $0.24 \mu\text{m}$  diameter with (■) 10%, (▲) 20%, (▼) 30% standard deviation.

for systems where fracture is dominated by the effects of particle/particle contacts the model will not be applicable. In particular, the model will fail for materials that are very brittle in nature because a continuous phase is unlikely to form in these systems during compaction.

### Acknowledgement

The authors thank Professor K. B. Broberg for his invaluable advice.

### References

1. A. B. MASHADI and J. M. NEWTON, *J. Pharm. Pharmacol.* **39** (1987) 961.
2. R. J. ROBERTS and R. C. ROWE, *Int. J. Pharm.* **52** (1989) 213.
3. P. YORK, F. BASSAM, R. C. ROWE and R. J. ROBERTS, *ibid.* **66** (1990) 143.
4. R. J. ROBERTS, R. C. ROWE and P. YORK, *ibid.* (1992) in press.
5. A. B. MASHADI and J. M. NEWTON, *J. Pharm. Pharmacol.* **40** (1988) Suppl. 120 p.
6. K. B. BROBERG in *Advances in Constitutive Laws for Engineering Materials*, edited by F. Jinghong and S. Murakami, Vol. 1, Pergamon, Oxford, 1989 pp. 255–358.
7. K. B. BROBERG, *Int. J. Fract.* **42** (1990) 277.
8. R. C. ROWE and R. J. ROBERTS, *Powder Technol.* submitted.
9. K. B. BROBERG, personal communication (1990).
10. H. GUCLUYILDIZ, G. S. BANKER and G. E. PECK, *J. Pharm. Sci.* **66** (1977) 407.
11. K. RIDGWAY, E. SHOTTEN and J. GLASBY, *J. Pharm. Pharmacol.* **21** (1969) Suppl. 19S.
12. R. J. ROBERTS, R. C. ROWE and P. YORK, *Powder Technol.* **65** (1991) 139.
13. K. RIDGWAY, M. E. AULTON and P. H. ROSSER, *J. Pharm. Pharmacol.* **22** (1970) 70S.
14. R. C. ROWE and R. J. ROBERTS, *Int. J. Pharm.* **78** (1992a) 49.
15. *Idem, ibid.* **86** (1992) 49.

Received 1 December  
and accepted 8 December 1992